Central exclusive production of quarkonium at LHCb

Xiaolin Wang
South China Normal University

第四届LHCb前沿物理研讨会
2024年7月29日·烟台

Xiaolin Wang
xiaolin.wang@cern.ch

Ultra-peripheral PbPb Collisions

- **Ultra-Peripheral Collisions(UPCs):**

  - Two incoming nuclei bypass each other with an impact parameter greater than the sum of their radii.
  - Reactions in which two ions interact via their cloud of semi-real photons.
  - The photon-induced interactions are enhanced by the strong electromagnetic field of the nucleus.
  - Photon-induced quarkonium production: A $q\bar{q}$ loop created by the photon interaction with a pair of gluon exchange (pomeron) to produce a quarkonium($c\bar{c}, b\bar{b}$).
  - Non-resonant background: $\gamma\gamma \rightarrow \mu^{+}\mu^{-}$.

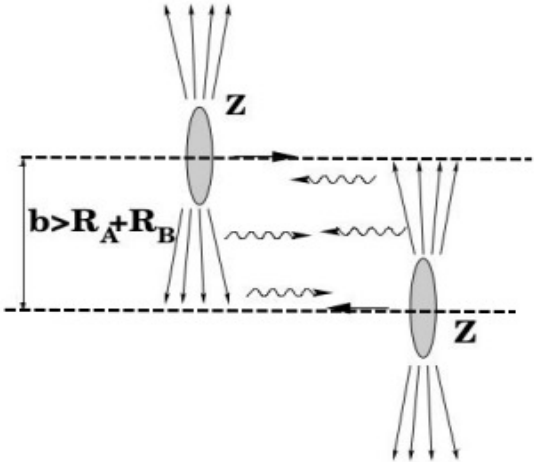

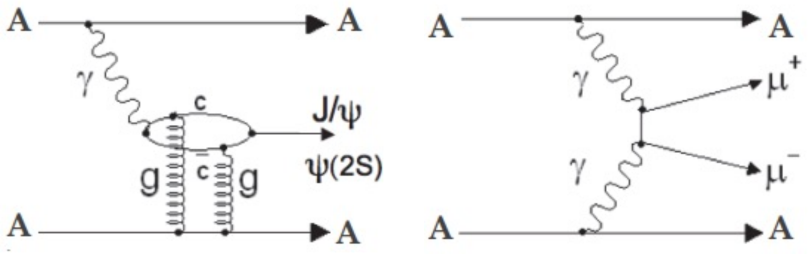

J/ψ production in UPC

- Coherent J/ψ production, photon interacts with a pomeron emitted by the entire nucleus.
- Incoherent J/ψ production, the photon interacts with a pomeron emitted from a single nucleon within the target nucleus.
- J/ψ from the feed-down of coherent and incoherent ψ(2S) production.
- Study of coherent charmonium production could constrain the gluon Parton Distribution Functions in nuclei.
- The ratio of J/ψ and ψ(2S) is helpful to constrain the choice of the vector meson wave function in dipole scattering models. [e.g. PLB 772 (2017) 832; PRC (2011) 011902]

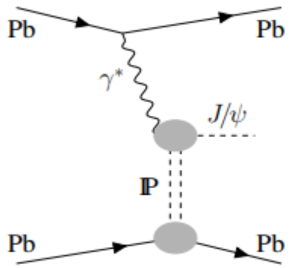

Coherent J/ψ production

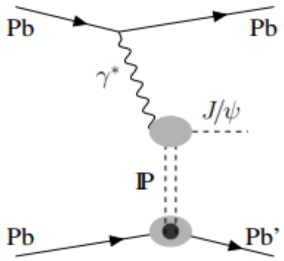

Incoherent J/ψ production

LHCb Detector

- LHCb detector is **a single-arm forward spectrometer** fully instrumented in unique kinematic coverage: **2<η<5**.
- A high precision detector with excellent particle identification, precise vertex and track reconstruction.

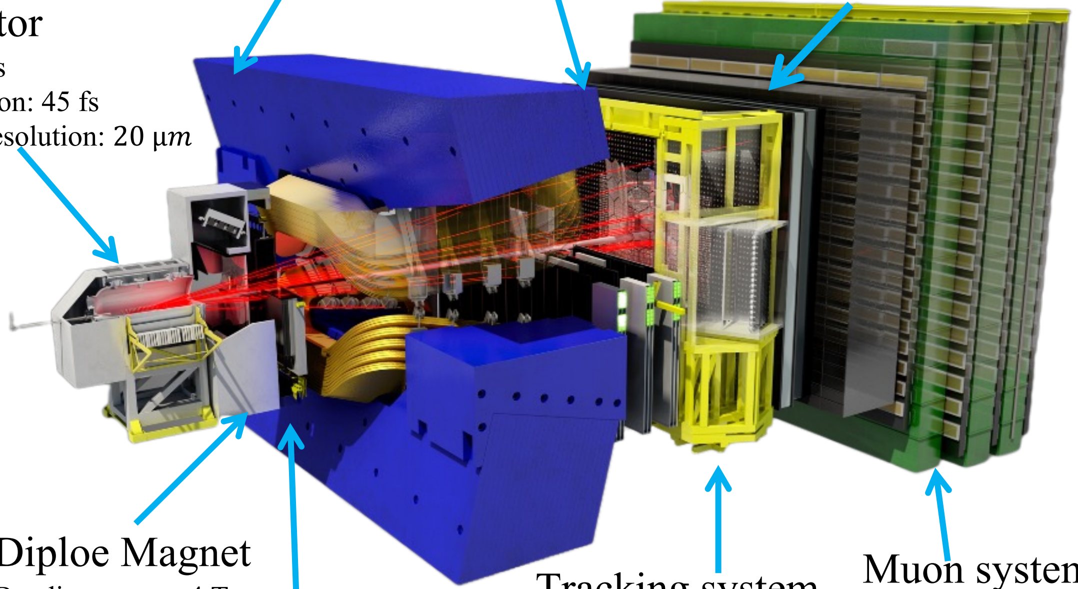

[Int. J. Mod. Phys. A 30, 1530022 (2015)]

Event selection

- Dataset: J/ψ → $\mu^+\mu^-$ and ψ(2S) → $\mu^+\mu^-$ events from PbPb collisions at $\sqrt{s}$ = 5.02TeV taken in 2018 with luminosity $228 \pm 10\ \mu b^{-1}$.
- Differential cross-sections of coherent J/ψ and ψ(2S) photon-production are measured as:

$$\frac{d\sigma_{\psi}^{coh}}{dx} = \frac{N_{\psi}^{coh}}{\mathcal{L} \times \varepsilon_{tot} \times \mathcal{B}(\psi \to \mu^+\mu^-) \times \Delta x}$$

- Event selection：
  - only two long tracks reconstructed for muons, with acceptance cuts:

$$2.0 < \eta^{\mu^{\pm}} < 4.5,\ p_T^{\mu^{\pm}} > 700MeV,$$
$$p_T^{\mu^+\mu^-} < 1GeV,\ |\Delta\phi_{\mu^+\mu^-}| > 0.9\pi$$

  - HeRSCheL detector is used to further purify the selection. [2018 JINST 13 P04017]

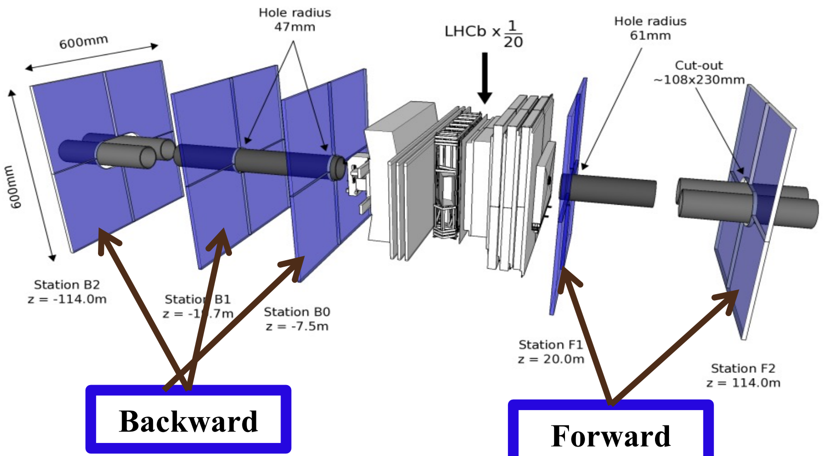

Signal extraction

JHEP 06 (2023) 146

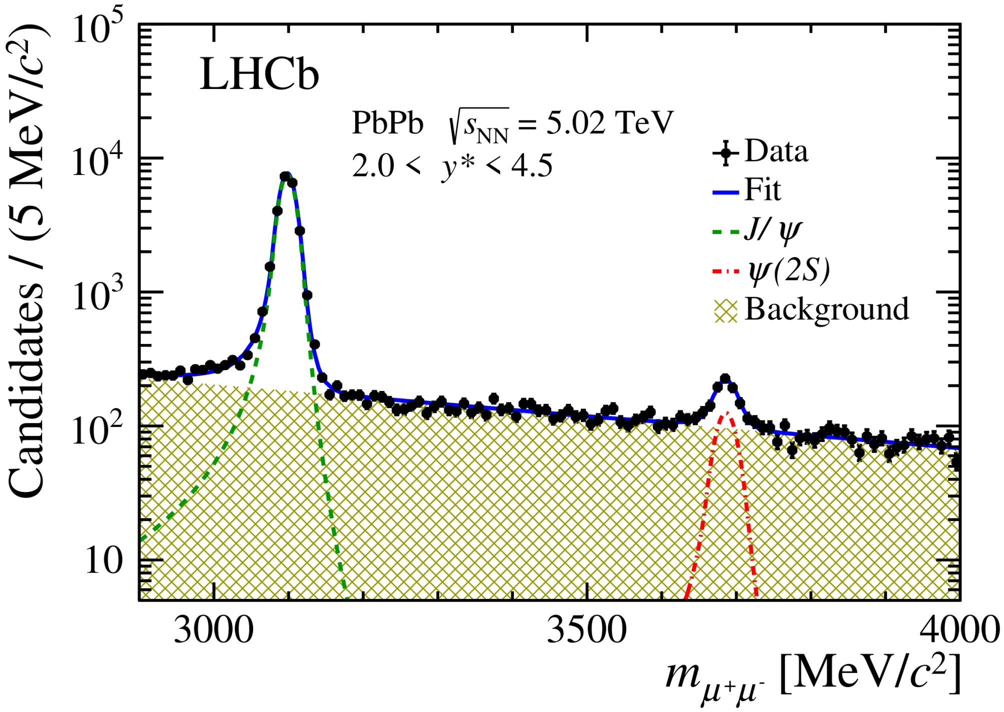

- Signal extraction step1: Charmonium yields are extracted from dimuon massfit.
  - Double-sided crystal ball function for the J/ψ and ψ(2S) yields.
  - Exponential function for the non-resonant background are extracted from dimuon massfit.

Signal extraction

JHEP 06 (2023) 146

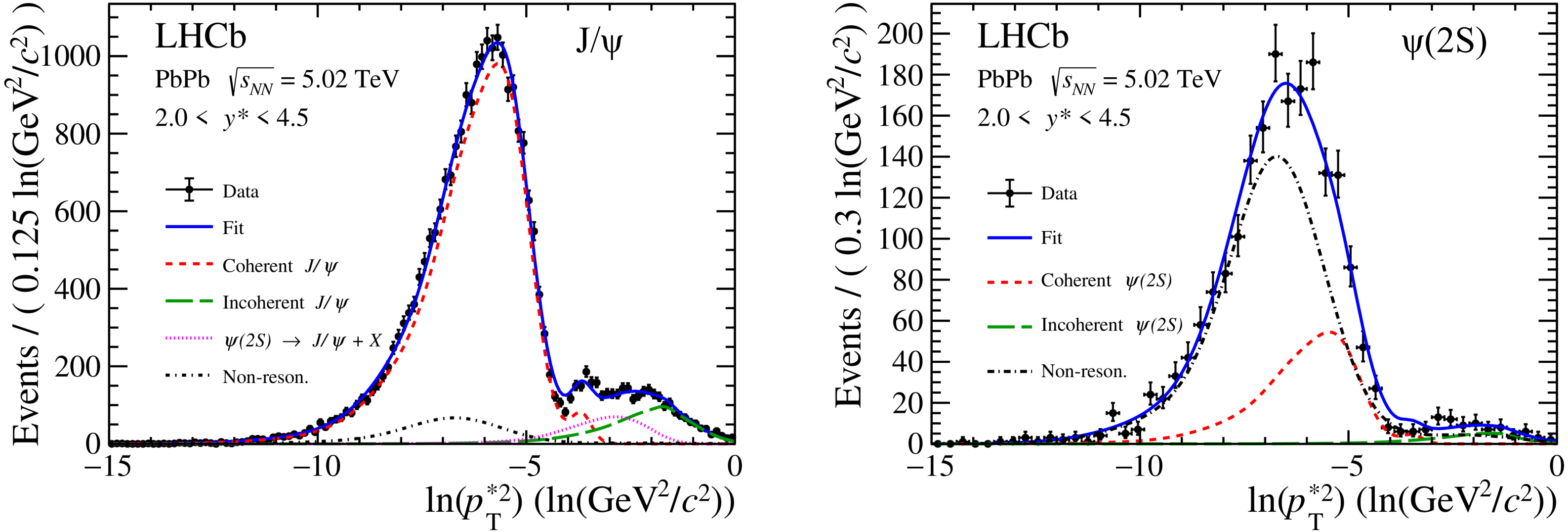

- Signal extraction step2: Coherent component is extracted from a $\ln(p_T^2)$ fit.
- All signal pdfs are estimated using the STARLight generator and the LHCb detector simulation.
- The shape of background taken from the side-band method, then the normalization is fixed from mass fit.

Cross-sections in rapidity

- The most precise coherent J/ψ production measurement in PbPb UPC in forward rapidity to date.
- The high precision LHCb data are of great value in theoretical model fine-tuning.
- Compare to most recent theoretical calculations:
  - p-QCD calculations: include new NLO p-QCD calculation PDF uncert. and factorization scale uncert.
  - Color-dipole models: draw different model tuning options as theoretical variations.

JHEP 06 (2023) 146

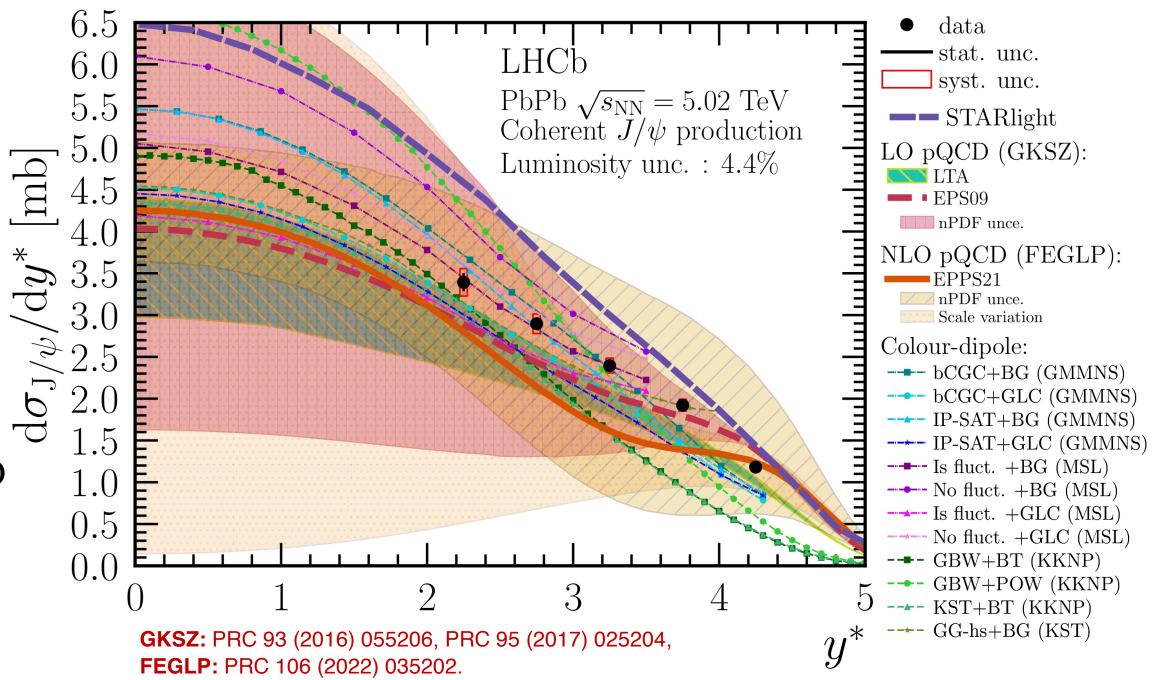

GKSZ: PRC 93 (2016) 055206, PRC 95 (2017) 025204,
FEGLP: PRC 106 (2022) 035202.
GMMNS: PRD 96 (2017) 094027, EPJC 40 (2005) 519,
MSL: PLB 772 (2017) 832, PoS DIS2014 (2014) 069,
KKNP: PRD 107 (2023) 054005
CCK: PRC 97 (2018) 024901

Cross-sections in rapidity

- The first precise coherent ψ(2S) production measurement in PbPb UPC in forward rapidity at LHC.
- Compare to most recent theoretical calculations of p-QCD calculations and color-dipole models.

GKSZ: PRC 93 (2016) 055206, PRC 95 (2017) 025204,
GMMNS: PRD 96 (2017) 094027, EPJC 40 (2005) 519,
MSL: PLB 772 (2017) 832, PoS DIS2014 (2014) 069,
KKNP: PRD 107 (2023) 054005
CCK: PRC 97 (2018) 024901

JHEP 06 (2023) 146

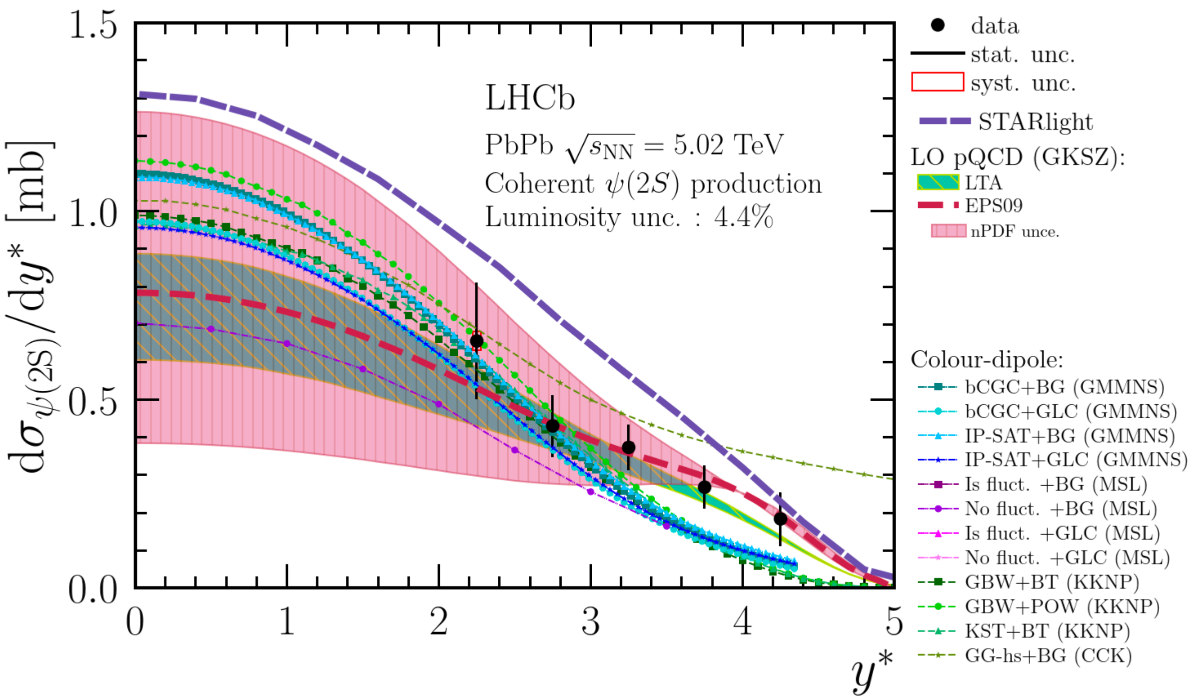

Cross-sections in rapidity

- The first cross-section ratio between coherent J/ψ and ψ(2S) vs. rapidity measurement in forward rapidity region at LHC.
- Compare to most recent theoretical calculations of p-QCD calculations and color-dipole models.

GKSZ: PRC 93 (2016) 055206, PRC 95 (2017) 025204,
GMMNS: PRD 96 (2017) 094027, EPJC 40 (2005) 519,
MSL: PLB 772 (2017) 832, PoS DIS2014 (2014) 069,
KKNP: PRD 107 (2023) 054005
CCK: PRC 97 (2018) 024901

JHEP 06 (2023) 146

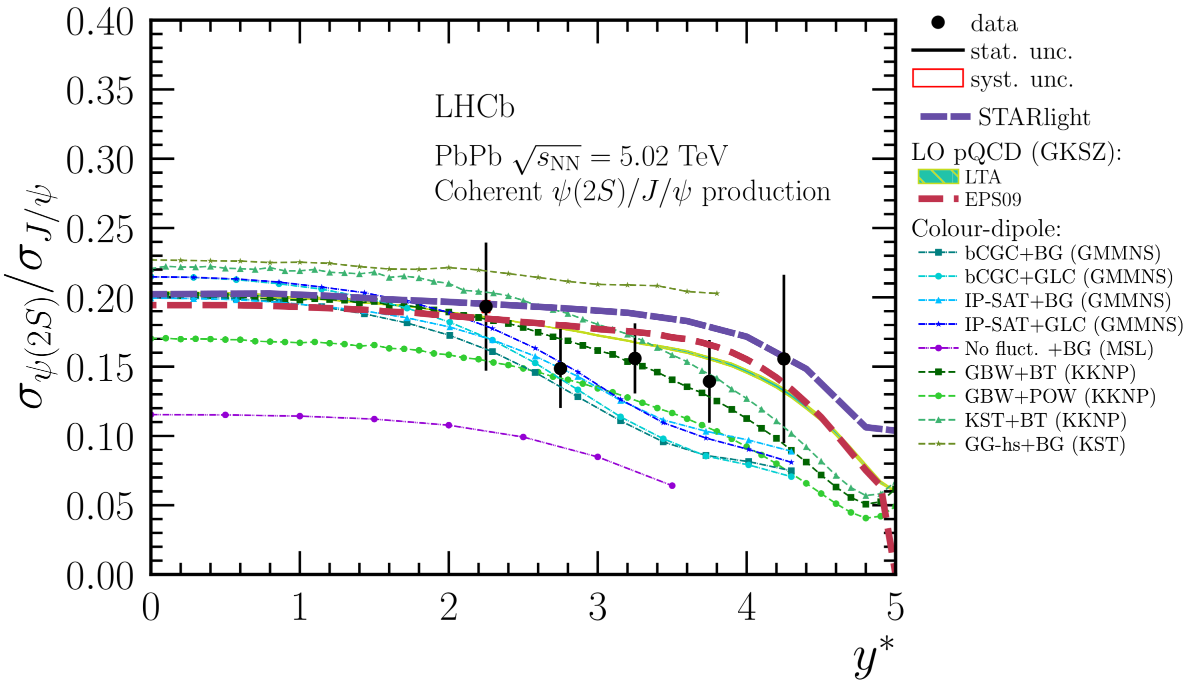

Cross-sections in p_T

JHEP 06 (2023) 146

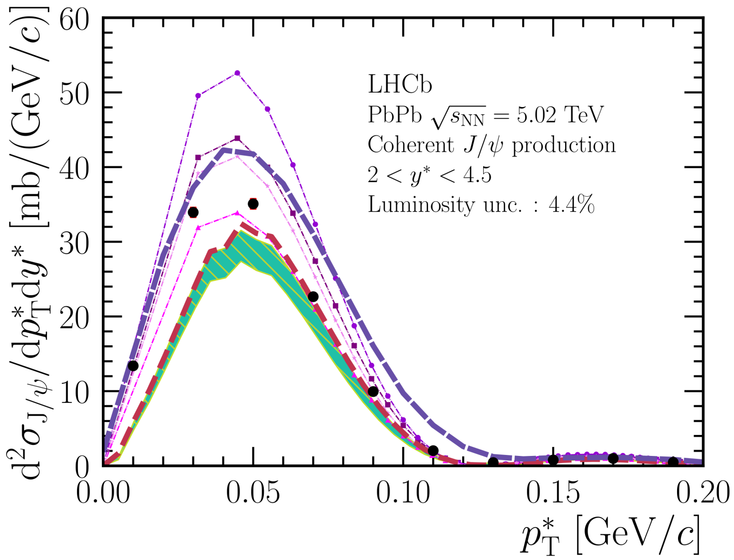

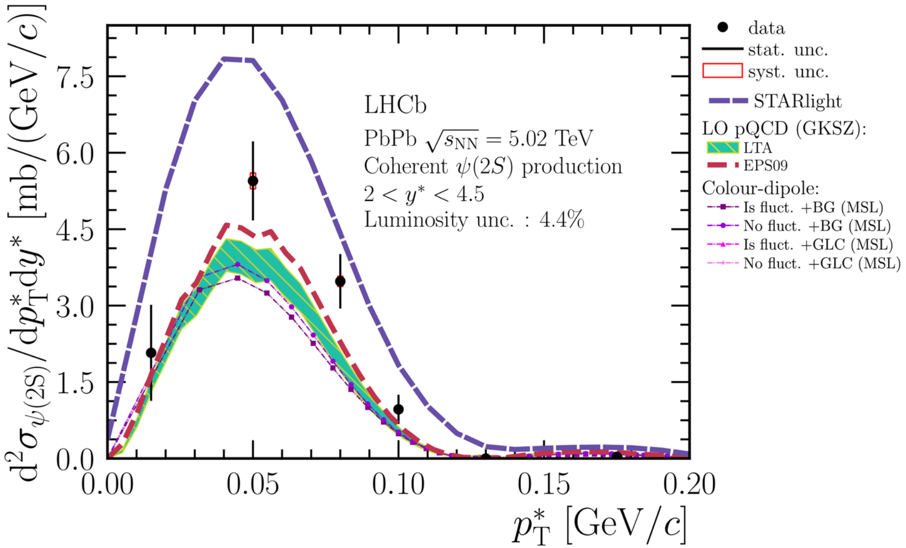

GKSZ: PRC 93 (2016) 055206, PRC 95 (2017) 025204,
MSL: PLB 772 (2017) 832, PoS DIS2014 (2014) 069,

- The first coherent J/ψ and ψ(2S) production measurement in p_T in PbPb UPC.
- Compare to most recent theoretical calculations of p-QCD calculations and color-dipole models.

Compare with other results

JHEP 06 (2023) 146

- Comparison with the coherent J/ψ production measurement with LHCb 2015, ALICE and CMS results.
  - The J/ψ measurement is compatible with LHCb2015, ALICE and CMS results.
  - The compatibility between the new results and 2015 measurement is about 2σ.

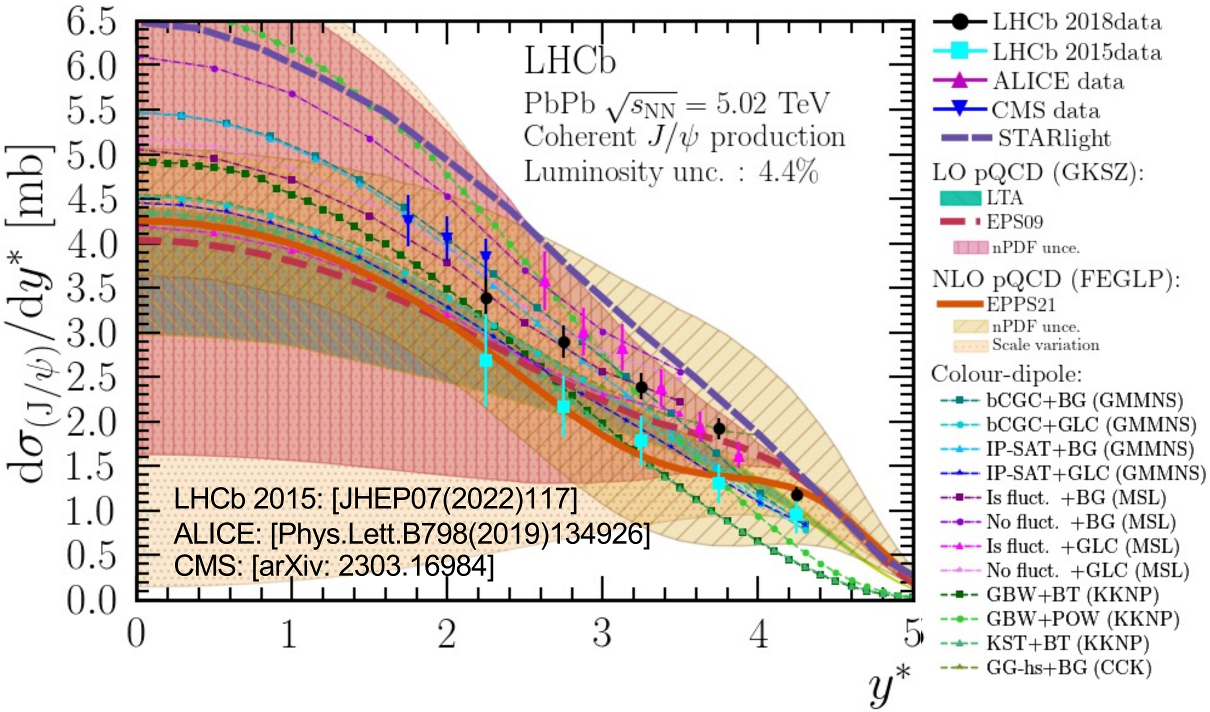

Conclusion

- Measurements of exclusive coherent J/ψ and ψ(2S) production and their cross-section ratio in UPC PbPb collisions using 2018 dataset. JHEP 06 (2023) 146
  - The most precise coherent J/ψ production measurement in forward rapidity region in PbPb UPC to date.
  - The first coherent ψ(2S) measurement in forward rapidity region in PbPb UPC at LHC.
  - The first measurement about coherent J/ψ and ψ(2S) production cross-sections vs. p_T in PbPb UPC.

- The results are compatible with current theoretical predictions, providing strong constraints for the fine-tuning of the different models.

- More results are ongoing： $c\bar{c}$, $b\bar{b}$, K^+K^-, $\pi\pi$, ϕ, etc…

CEP collisions

- **Central Exclusive Production(CEP):**
  - p + p → p + X + p, incoming protons do not dissociate.
- **Study of CEP of $\Upsilon(nS)$ in the dimuon decay mode:**
  - The study of CEP $\Upsilon(nS)$ is an essential tool to understand the low-x physics(down to 10^{-5}) and also to investigate the gluon PDF in this regime.
  - The measurement of CEP $\Upsilon(nS)$ production could test $\Upsilon(nS)$ wave function models.
  - Improve the accuracy on the previous reported result.

JHEP 1509, 084 (2015)

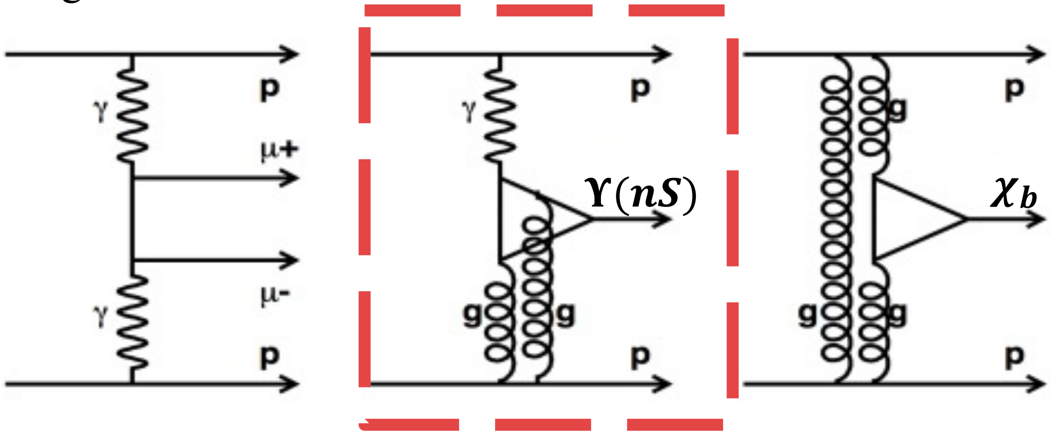

Observables and selections

- Datasets

Table 21: Summary of the integrated luminosity, list the good runs and bad runs separately, $4.691 fb^{-1}$ in total.

Lumi.	2016		2017		2018	
	MagUp	MagDown	MagUp	MagDown	MagUp	MagDown
$\mathcal{L}_{int}^{good}(pb^{-1})$	496 ± 10	636 ± 13	672 ± 13	646 ± 13	923 ± 19	804 ± 16
$\mathcal{L}_{int}^{bad}(pb^{-1})$	44 ± 4	59 ± 6	58 ± 6	87 ± 9	115 ± 11	152 ± 15
$\mathcal{L}_{int}^{tot}(pb^{-1})$	540 ± 11	695 ± 14	730 ± 15	732 ± 15	1038 ± 22	956 ± 22

- Production cross-sections in $2 \leq y(\Upsilon(1,2,3S)) \leq 4.5$.
- Differential cross-sections for $\Upsilon(1,2S)$: [2.0, 3.0], [3.0, 3.5], [3.5, 4.5].

$$\frac{d\sigma_{\Upsilon(nS)}}{dy} = \frac{N_{\Upsilon(nS)}}{\mathcal{L}_{tot}^{eff} \times \varepsilon_{\text{tot}} \times \mathcal{B}(\Upsilon(nS) \to \mu^+\mu^-) \times \Delta y}$$

Variable	Requirement
Geometrical acceptance selection	
muon $\eta_{\mu^\mp}$	$2.0 < \eta_{\mu^\mp} < 4.5$
Selection cuts	
nLongTracks	$= 2$
nVeloTracks	$= 2$
dimuon ${p_{\mathrm{T}}}^2$	$< 2\,\mathrm{GeV}$
Trigger Selection	
L0	L0Muon, lowMult||L0DiMuon, lowMult
HLT1	Hlt1LowMultMuon
HLT2	Hlt2LowMultDiMuon
PID Selection	
muplus_isMuon	$= 1$
muminus_isMuon	$= 1$
ProbNNmu*(1-ProbNNk)*(1-ProbNNpi)	> 0.05
Herschel Selection	
$\ln({\chi^2}_{\mathrm{HRC}})$	≤ 5.5
sum of HRC ADC hits	$\sum_i S_i < 750$
Mass window Selection	
$m_{\mu^\pm}$ (for mass fit)	$9.0 < m_{\mu^\pm} < 10.8$ GeV
$m_{\mu^\pm}$ (for $p_{\mathrm{T}\Upsilon(1S)}$ fit)	$\lvert m_{\mu^\pm} - m_{\Upsilon(1S)}\rvert < 100$ MeV
$m_{\mu^\pm}$ (for $p_{\mathrm{T}\Upsilon(2S)}$ fit)	$\lvert m_{\mu^\pm} - m_{\Upsilon(2S)}\rvert < 120$ MeV
$m_{\mu^\pm}$ (for $p_{\mathrm{T}\Upsilon(3S)}$ fit)	$\lvert m_{\mu^\pm} - m_{\Upsilon(2S)}\rvert < 150$ MeV

Invariant massfit

- Fit to Invariant mass spectrum in [9000, 10800] MeV/c^2
- Double-sided Crystal Ball function for the mass peaks.
- Exponential function for the non-resonant background.
  - continuum $\gamma\gamma \rightarrow \mu^+\mu^-$
  - part of inelastic pp bkg
- Results of massfit

Table 9: Total $\Upsilon(nS)$ and non-resonant background yields from the invariant mass fits in different rapidity intervals.

Interval	$N^{tot}_{\Upsilon(1S)}$	$N^{tot}_{\Upsilon(2S)}$	$N^{tot}_{\Upsilon(3S)}$	$N^{bkg}_{\Upsilon(1S)}$	$N^{bkg}_{\Upsilon(2S)}$	$N^{bkg}_{\Upsilon(3S)}$
$2.0 \leq y \leq 4.5$	532 ± 29	156 ± 22	101 ± 19	187 ± 28	170 ± 24	178 ± 21
$2.0 \leq y \leq 3.0$	214 ± 17	54 ± 12	36 ± 13	67 ± 16	63 ± 13	69 ± 15
$3.0 < y \leq 3.5$	179 ± 17	54 ± 13	37 ± 13	74 ± 17	70 ± 14	75 ± 15
$3.5 < y \leq 4.5$	141 ± 15	45 ± 10	29 ± 8	43 ± 14	37 ± 10	34 ± 9

LHCb-ANA-2021-059

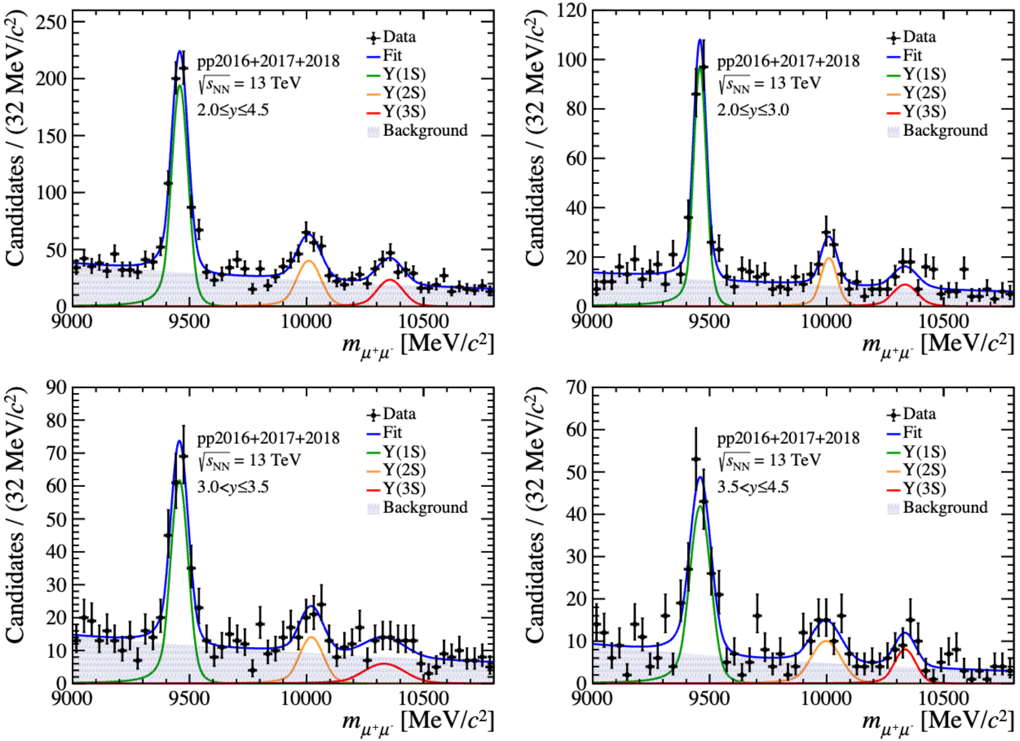

Figure 3: Invariant mass spectrum for the combined datasets of 2016, 2017, and 2018(black dots) with offline selections applied.

$\Upsilon(1S)$ lnpt2fit

- Fit to lnp_T^2 spectrum for $\Upsilon(1S)$ in [-10, 1] MeV^2/c^2
- Fix the shape of the signal lnp_T^2 distribution from official MC.
- Fix the shape of the χ_b feeddown lnp_T^2 distribution from $\chi_{b0}(3P) \to \Upsilon(1S) + \gamma$ by SuperChic4.2
- Fix the shape of non-resonant bkg by side-band method, the norm. by massfit.
- Need to consider the inelastic pp bkg in the mass peak.

Interval	$N^{excl}_{\Upsilon(1S)}$	$N^{excl}_{\Upsilon(2S)}$	$N^{excl}_{\Upsilon(3S)}$
$2.0 < y < 4.5$	414 ± 26	113 ± 17	77 ± 15
$2.0 < y < 3.0$	159 ± 16	43 ± 10	31 ± 9
$3.0 < y < 3.5$	131 ± 15	42 ± 10	30 ± 9
$3.5 < y < 4.5$	125 ± 14	28 ± 8	17 ± 7

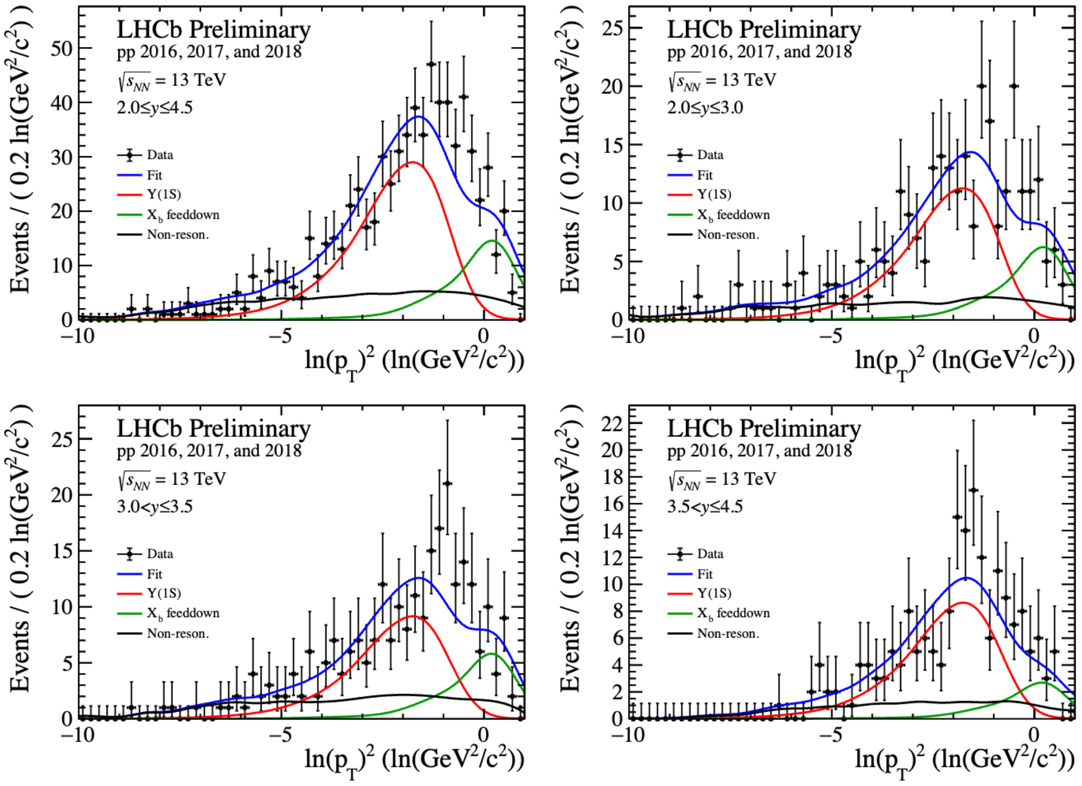

Efficiency and uncertainty

- The efficiencies in the analysis are:
  - For 2018:

Rapidity bins	$2.0 < y < 4.5$	$2.0 < y < 3.0$	$3.0 < y < 3.5$	$3.5 < y < 4.5$
$\epsilon_{acceptance}$	0.449 ± 0.003	0.389 ± 0.005	0.739 ± 0.011	0.361 ± 0.004
$\epsilon_{tracking}$	0.7626 ± 0.0003	0.7794 ± 0.0006	0.7709 ± 0.0007	0.7335 ± 0.0007
$\epsilon_{trigger}$	0.7926 ± 0.0005	0.7406 ± 0.0008	0.7915 ± 0.0008	0.8594 ± 0.0008
$\epsilon_{selection}$	0.9885 ± 0.0001	0.9890 ± 0.0002	0.9881 ± 0.0002	0.9885 ± 0.0002
ϵ_{PID}	0.9992 ± 0.0000	0.9990 ± 0.0001	0.9991 ± 0.0001	0.9996 ± 0.0000
$\epsilon_{Herschel}$	0.85 ± 0.01	0.85 ± 0.01	0.85 ± 0.01	0.85 ± 0.01
ϵ_{total}	0.2278 ± 0.004	0.1886 ± 0.004	0.3784 ± 0.008	0.1911 ± 0.004

- The sources of sys. uncertainty are:

Table 11: Summary of the systematic uncertainties.

Source	Relative uncertainty [%] $\sigma_{\Upsilon(1S)}$
Tracking efficiency	0.04–0.1
Trigger efficiency	0.04–0.1
HERSCHEL efficiency	1.522
Non-resonant bkg. estimation	5.5
Feed-down Chib bkg. shape	8.05
Branching fraction	2.016
Luminosity	1.234

Cross section

➢ The preliminary $\Upsilon(1S)$ cross-section :

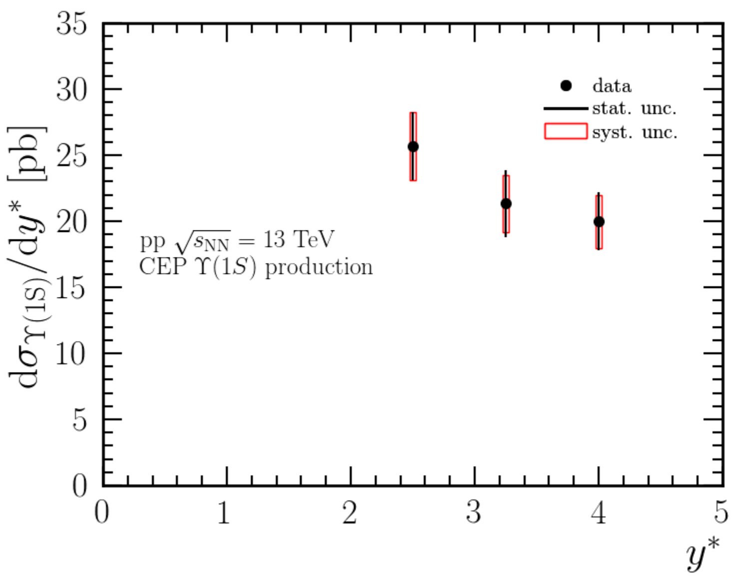

Table 12: The differential cross-section for CEP $\Upsilon(1S)$production as a function of y^*.

Interval	$d\sigma^{coh}_{\Upsilon(1S)}/dy^*$ [pb]	Uncertainties [pb]			
		Stat.	Syst.	Lumi.	Total
$2.0 < y^* < 3$	22.050	2.495	2.239	0.272	3.364
$3.0 < y^* < 3.5$	17.639	2.326	1.796	0.218	2.947
$3.5 < y^* < 4.5$	14.635	1.937	1.483	0.181	2.446
$2.0 < y^* < 4.5$	44.611	3.235	4.503	0.551	5.572

Rapidity bins	$2.0 < y < 4.5$	$2.0 < y < 3.0$	$3.0 < y < 3.5$	$3.5 < y < 4.5$
$Stat.unce(\%)$	7.251	11.316	13.187	13.234
$Sys.unce(\%)$	10.094	10.154	10.182	10.133
$Branching.unce(\%)$	2.016	2.016	2.016	2.016
$Lumi.unce(\%)$	1.234	1.234	1.234	1.234

Now：

$$\frac{d\sigma_{\Upsilon(nS)}}{dy} = \frac{N_{\Upsilon(nS)}}{\mathcal{L}^{eff}_{tot} \times \varepsilon_{\rm tot,2018} \times \mathcal{B}(\Upsilon(nS) \to \mu^+\mu^-) \times \Delta y}$$

Thanks!

Back up

HeRSCheL detector

[2018 JINST 13 P04017]

- HeRSCheL(**High Rapidity Shower Counters for LHCb**), is a set of plastic scintillators located in the LHC tunnel on both sides of the LHCb interaction point, in order to extend the pseudo-rapidity coverage of the LHCb in the high-rapidity regions either side of the interaction point.

- HeRSCheL detector extends the LHCb forward coverage up to a pseudo-rapidity of around 10.

- HeRSCheL detector is used to cut the component with large momentum, for example, the incoherent component.

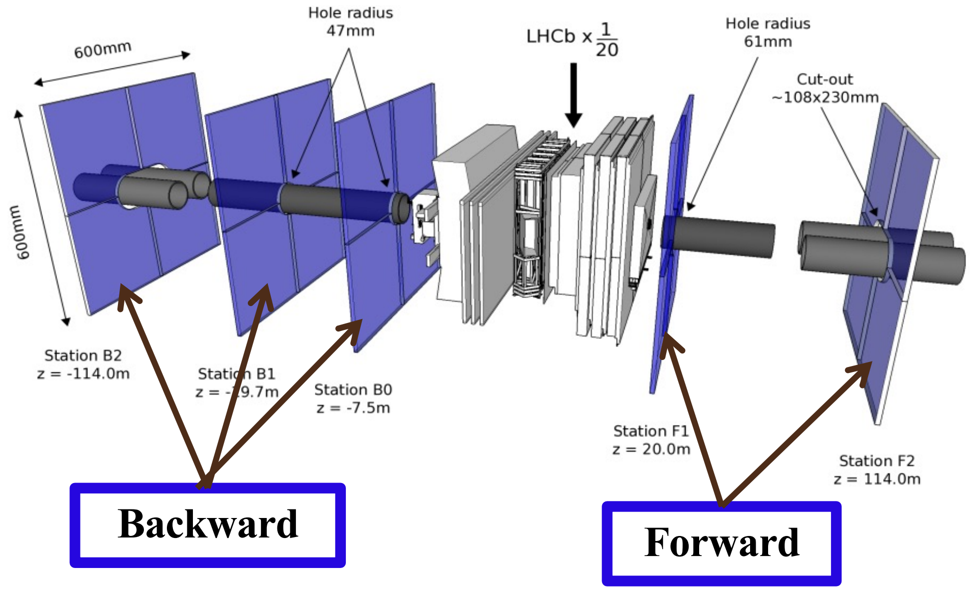

Cross-sections results

JHEP 06 (2023) 146

- Integrated cross-section and ratio (most precise measurements in the forward region at this moment):

$$\sigma^{coh}_{J/\psi} = 5.965 \pm 0.059(\text{stat}) \pm 0.232(\text{syst}) \pm 0.262(\text{lumi})\ \text{mb},$$
$$\sigma^{coh}_{\psi(2S)} = 0.923 \pm 0.086(\text{stat}) \pm 0.028(\text{syst}) \pm 0.040(\text{lumi})\ \text{mb},$$
$$\sigma^{coh}_{\psi(2S)}/\sigma^{coh}_{J/\psi} = 0.155 \pm 0.014(\text{stat}) \pm 0.003(\text{syst}).$$

- Systematic uncertainties:

Source	Relative uncertainty [%]	
	$\sigma^{coh}_{J/\psi}$	$\sigma^{coh}_{\psi(2S)}$
Tracking efficiency	0.5–2.0	0.5–2.0
PID efficiency	0.9–1.6	0.9–1.6
Trigger efficiency	2.7–3.7	2.1–2.5
HeRSChel efficiency	1.4	1.4
Background estimation	1.2	1.2
Signal shape	0.04	0.04
Momentum resolution	0.9–34	1.3–27
Branching fraction	0.6	2.1
Luminosity	4.4	4.4

Backgrounds under mass peak

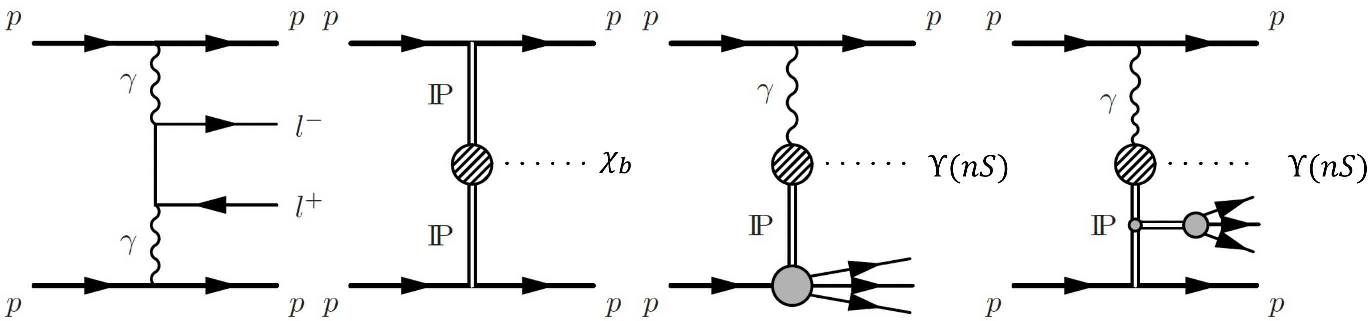

(a) Continuum $\ell^+\ell^-$ (b) Exclusive χ_{bJ} (c) Proton dissociation (d) Gluon radiation

- Feed-down $\chi_{bJ} \to \Upsilon\gamma$ decays

  $\chi_{b0,1,2}(1P), \chi_{b0,1,2}(2P), \chi_{b0,1,2}(3P) \to \Upsilon(1S)\gamma$, $\chi_{b0,1,2}(2P), \chi_{b0,1,2}(3P) \to \Upsilon(2S)\gamma$, $\chi_{b0,1,2}(3P) \to \Upsilon(3S)\gamma$.

- Non-resonant production of $\mu^+\mu^-$

  Can be determined from a fit to the dimuon invariant mass distribution.

- Inelastic interaction

  Non-resonant part can be determined from a fit to the dimuon invariant mass distribution.

  Need to obtain the resonant part shape of inelastic pp bkg inside the mass peak.

- Example distribution in J/ψ case

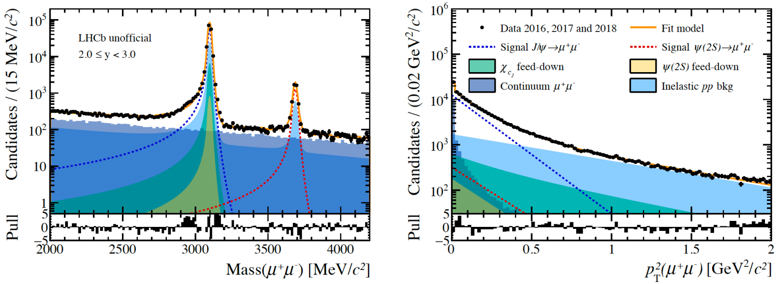

LHCb-ANA-2021-059

Previous studies at LHCb

- Exclusive $\Upsilon(nS)$ production in pp collisions at 7 and 8 TeV, using 2011 and 2012 datasets at LHCb.

[JHEP 1509, 084(2015)]

For $2 < y(\Upsilon(nS)) < 4.5$:

$$\sigma(pp \to p\Upsilon(1S)p) = 9.0 \pm 2.1 \pm 1.7\,\text{pb},$$
$$\sigma(pp \to p\Upsilon(2S)p) = 1.3 \pm 0.8 \pm 0.3\,\text{pb}, \quad \text{and}$$
$$\sigma(pp \to p\Upsilon(3S)p) < 3.4\,\text{pb at the 95\% confidence level},$$

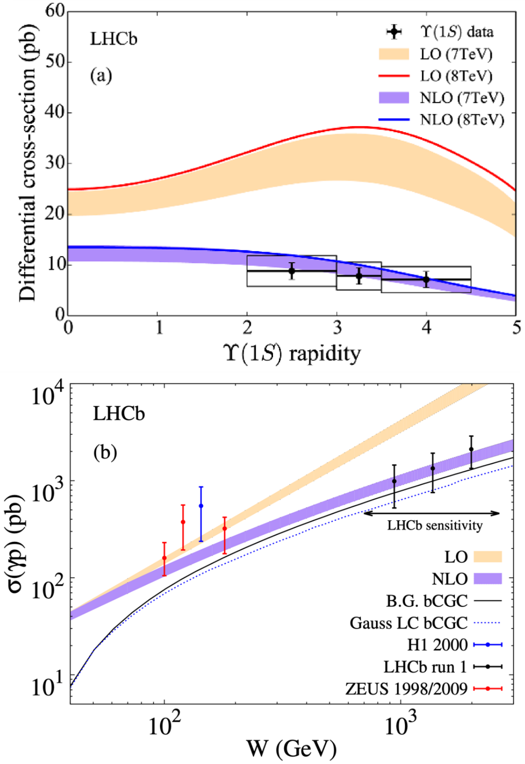

- CEP J/ψ and $\psi(2S)$ using 2016-18 datasets

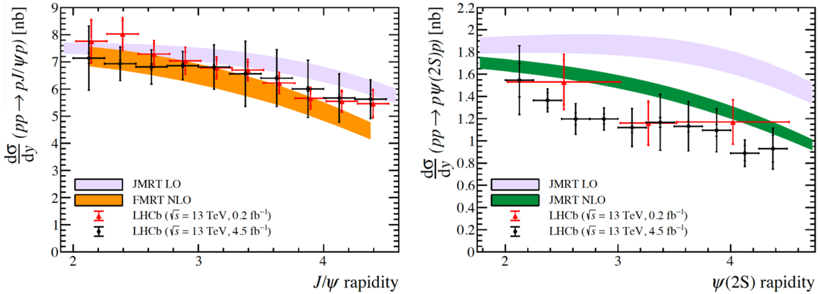

In review

$$\sigma_{J/\psi\to\mu^+\mu^-}(2 < \eta_{\mu^+\mu^-} < 4.5) = 431 \pm 2 \pm 24 \pm 13\,\text{pb},$$
$$\sigma_{\psi(2S)\to\mu^+\mu^-}(2 < \eta_{\mu^+\mu^-} < 4.5) = 10.2 \pm 0.2 \pm 0.6 \pm 0.3\,\text{pb},$$

LHCb-ANA-2021-059

$J/\psi, \psi(2S)$ Photo-production cross-section in CEP

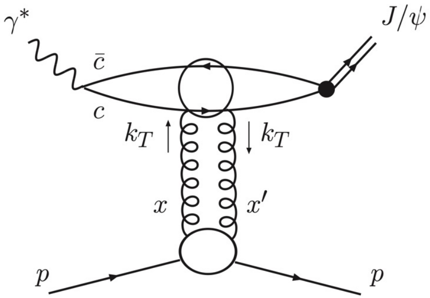

JHEP11(2013)085

photon energy
$k_\pm \equiv (M_\psi/2)e^{\pm y_\psi}$

Invariant mass of the photon-proton system
$W_\pm^2 = 2k_\pm\sqrt{s}$

External inputs

gap survivor   photon flux

Photoproduction result from H1(HERA)

parametrization = $a\left(\frac{W}{90\ \text{GeV}}\right)^\delta$

$$\sigma_{pp\to p\psi p} = r(W_+)\left(\frac{dn}{dk_+}\right)k_+\boldsymbol{\sigma_{\gamma p\to\psi p}(W_+)} + r(W_-)\left(\frac{dn}{dk_-}\right)k_-\,\sigma_{\gamma p\to\psi p}(W_-)$$

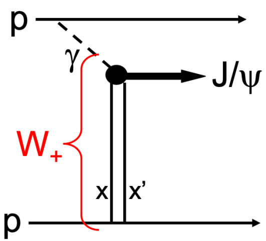

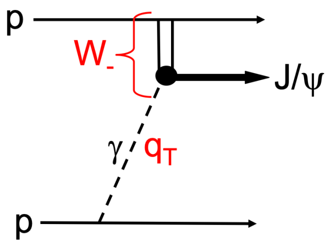

- $\sigma_{pp\to p\psi p}$(W) has contributions from photon coming from both forward and backward going proton in CMS
- **Goal:** Extract ψ photoproduction cross – section $\boldsymbol{\sigma_{\gamma p\to\psi p}(W)}$ from measured $\boldsymbol{\sigma_{pp\to p\psi p}(W)}$

$W^2 \equiv 2k\sqrt{s}$

Photoproduction cross-section